

**EFFECT OF CRYSTALLOGRAPHIC ORIENTATION ON MECHANICAL PROPERTIES  
OF STEEL SHEETS BY DEPTH SENSING INDENTATION**

BURIK Peter <sup>1</sup>, PEŠEK Ladislav <sup>2</sup>

<sup>1</sup>Technical University of Liberec, Faculty of Mechanical Engineering, Department of Material Science, Liberec, Czech Republic, EU, [peter.burik@tul.cz](mailto:peter.burik@tul.cz)

<sup>2</sup>Technical University of Košice, Faculty of Metallurgy, Department of Materials Science, Kosice, Slovakia, EU, [ladislav.pesek@tuke.sk](mailto:ladislav.pesek@tuke.sk)

**Abstract**

The macroscopic mechanical properties of steel are highly dependent upon microstructure, crystallographic orientation of grains and distribution of each phase present etc. Nanomechanical testing using depth sensing indentation (DSI) provides a straightforward solution for quantitatively characterizing each of phases in microstructure because it is very powerful technique for characterization of materials in small volumes. Measuring the local properties (indentation hardness  $H_{IT}$ , Young's modulus  $E_{IT}$ , indentation energy: total  $W$ , elastic  $W_{el}$ , plastic  $W_{pl}$ ) of each microstructure component separately in multiphase materials gives information that is valuable for the development of new materials and for modelling [1].

In this work, depth sensing indentation has been used to reveal mechanical properties of individual ferrite grains with different crystallographic orientations in various steel sheets. Electron backscatter diffraction (EBSD) analysis was used to determine the grain orientations, in which were made the nanohardness measurements.

**Keywords:** Berkovich diamond indenter, crystallographic orientation, hardness, Young's modulus, steel sheet

**1. INTRODUCTION**

Nanomechanical testing using depth sensing indentation (DSI) provides a straightforward solution for quantitatively characterization (indentation hardness  $H_{IT}$ , Young's modulus  $E_{IT}$ , indentation energy: total  $W$ , elastic  $W_{el}$ , plastic  $W_{pl}$ ) of each phases in microstructure because it is very powerful technique for characterization of materials in small volumes. The principal goal of this method is to extract mechanical properties from indenter load vs. depth of penetration profile [1, 2]. The most commonly used method is the Oliver and Pharr method (O&P). In the O&P analysis, the hardness,  $H_{IT}^{O\&P}$ , and Young's modulus,  $E_{IT}^{O\&P}$ , are determined from the load - depth curve. The hardness is defined as:

$$H_{IT}^{O\&P} = \frac{P_{max}}{A_p^{O\&P}} \tag{1}$$

where  $P_{max}$  is the maximum indentation load and  $A_p^{O\&P}$  is the projected contact area at  $P_{max}$ . The reduced Young's modulus  $E_r$  is derived from the relation:

$$E_r = \frac{\sqrt{\pi}}{2\beta} \frac{S}{\sqrt{A_p^{O\&P}}} \tag{2}$$

where  $S$  is the contact stiffness computed from the initial slope of the unloading curve at the  $P_{max}$ ,  $\beta$  is a constant that depends on the geometry of the indenter ( $\beta = 1.034$  for a Berkovich indenter) and  $E_r$  is the reduced modulus given by:

$$\frac{1}{E_r} = \frac{1-\nu_s^2}{E_{IT}^{O\&P}} + \frac{1-\nu_i^2}{E_i} \tag{3}$$

where  $\nu_s$  and  $\nu_i$  are the Poisson's ratios of the samples and the indenter, respectively, and  $E_{IT}^{O\&P}$  and  $E_i$  are the corresponding Young's modulus (for a diamond indenter,  $E_i = 1141$  GPa and  $\nu_i = 0.07$ ). From Eq. (2) and Eq. (3) can be the Young's modulus  $E_{IT}^{O\&P}$  determined.

The projected contact area  $A_p^{O\&P}$  is calculated by evaluating an empirically determined indenter shape function  $A_p^{O\&P} = f(h_c^{O\&P})$ . For an ideal Berkovich indenter, it is given by:

$$A_p^{O\&P} = 24.56h_c^{2\ O\&P} \quad (4)$$

where  $h_c^{O\&P}$  is the contact depth between material and indenter at the  $P_{max}$ , which is also deduced from the load - depth curve using:

$$h_c^{O\&P} = h_{max} - \varepsilon \frac{P_{max}}{S} \quad (5)$$

where  $\varepsilon$  is a constant related to the geometry of the indenter (for a Berkovich indenter,  $\varepsilon = 0.75$ ) and  $h_{max}$  is the maximum indentation depth [3]. In this paper, we present study in which hardness and Young's modulus of steel sheets were measured by DSI method at the grain scale. We performed the grid indentation method [4, 5] on an area containing several grains with different crystallographic orientation which was simultaneously characterized by electron backscattering diffraction (EBSD).

## 2. MATERIAL AND METHODS

The materials used in this study are steel sheets:

- (i) XSG steel - **interstitial free steel** (ferrite microstructure). The mean size of the ferrite grain is 19  $\mu\text{m}$  (**Fig. 1a**).
- (ii) HR 45 steel - microalloyed steel (ferrite-pearlite microstructure). The mean size of the ferrite and pearlite grain is 7.9  $\mu\text{m}$  and 3.9  $\mu\text{m}$ , respectively. The volume fraction of pearlite phase is 14 % (**Fig. 1b**).

Chemical composition, mechanical properties and thickness  $t$  of the steels used are in **Table 1**. Microstructure was mechanical polished down to 0.25  $\mu\text{m}$  and subsequent chemical-mechanical polished to reduce local work hardening in the near-surface region to a minimum.

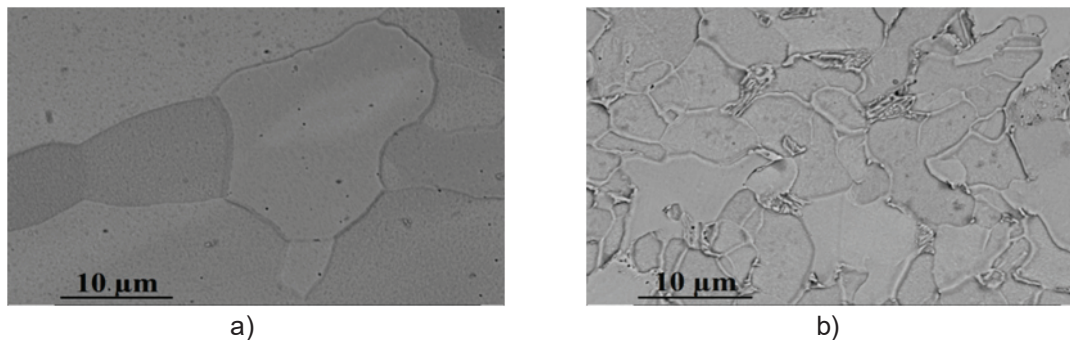


**Fig. 1** Microstructure of investigated steels, a) XSG, b) HR 45

**Table 1** Chemical composition [wt. %], mechanical properties and thickness  $t$  of investigated steels

Steel	C	Mn	V	S	P	$R_{p0.2}$ [MPa]	$R_m$ [MPa]	$A_{80}$ [%]	HV 1	n	t [mm]
XSG	0.0013	0.082	0.002	0.0105	0.011	177	286	47.2	120	0.211	1.95
HR 45	0.156	0.654	0.002	0.004	0.013	360 $R_e$	449	27	179	0.139	1.80

Indentation were carried out in the 10 x 11 matrix with a CSM instrument equipped with a Berkovich diamond indenter at a constant loading rate of 400 mN / min from 0 to the maximum force 5 mN, with 10 s hold period and constant unloading, the distance between the indentations was 8  $\mu\text{m}$ . The load - depth curve were analyzed using the O&P analysis. After indentations, the indent location was observed via scanning electron microscope and the crystallographic orientation of grains with individual orientations was examined by means

of EBSD method. High resolution EBSD images were prepared on an area  $\sim 100 \times 100 \mu\text{m}$  using a step size of 300 nm and applying a tilt angle of  $70^\circ$ . The obtained EBSD data were analyzed by HKL Channel 5 software. The program describes the orientation by using Euler angles ( $\varphi_1$ ,  $\Phi$ ,  $\varphi_2$ ), **Fig. 2**. Due to the assumed rotational symmetry of body centred cubic (BCC) grid, the relevant angle is only  $\varphi_2$  in the present analysis.  $\varphi_2$  ranges from  $0^\circ$  up to  $45^\circ$  to characterise the orientation dependence of hardness and Young's modulus. Namely,  $\varphi_2$  is the angle of the crystal rotation from plane (001) to plane (101). Pairing of the measured mechanical properties to the corresponding crystallographic orientation of each indent was carried out so that the indents located inside the grains were taken into account, those which corresponded to the close grain boundary area of crystals (closer than the diameter of an indent) were neglected from the evaluation. Effect of crystallographic orientation on mechanical properties in HR 45 steel was determined only for ferrite component.

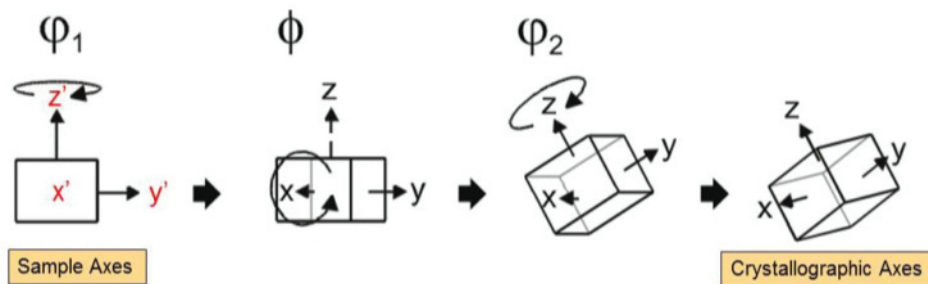


**Fig. 2** Formation of Euler angles [6]

### 3. RESULTS AND DISCUSSION

**Fig. 3** shows the IPF (Inverse Pole Figure) map which describes the crystallographic orientation of detected grains of XSG steel. IPF of the investigated area on which the nano-indentation tests were performed, practically completely covers the whole possible grain orientations, **Fig. 3a**. In order to study the differences between crystallographic orientation and hardness and Young's modulus, respectively grains with different crystallographic orientations in the sheet plane ((001), (001), (111)) were chosen. The hardness and Young's modulus are dependent on crystallographic orientation, **Fig. 3b**, **Fig. 3c**. The hardness and Young's modulus is substantially lower in the (001) plane than in plane (101) and (111). The hardness of the ferrite grain in plane (001) is lower about 5 % in XSG steel and about 4 % in HR 45 steel than in plane (101). Young's modulus of the ferrite grain in (001) plane is lower about 4 % in XSG steel and 5 % in HR 45 than in plane (101).

Mechanical properties in individual crystallographic planes depend on the chemical composition and grain size. XSG steel with coarse-grained microstructure has lower hardness (about 18 %) and Young's modulus (about 12 %) than HR 45 steel with fine-grained microstructure, **Table 2**. The values of mechanical characteristics of ferrite grain in different crystallographic plane have a high standard deviation due to:

- High surface roughness: for example - HR 45 steel  $R_a = 0.053 \pm 0.006 \mu\text{m}$ , the maximum depth in plane (100)  $h_{\text{max}} = 0.359 \pm 0.017 \mu\text{m}$ , in plane (101)  $h_{\text{max}} = 0.346 \pm 0.019 \mu\text{m}$  and in plane (111)  $h_{\text{max}} = 0.351 \pm 0.013 \mu\text{m}$ .
- Different indentation distance from the grain boundary.
- Roughness of the soft phase and that of hard phase is not equal, slip of the indenter can occur.
- Depth of the indented area is unknown, it is likely that measured hardness value of hard component is affected by the soft component which is under indented hard grain and opposite the soft component may be affected by the hard one lying under that. Therefore the hardness value of hard component may be shifted to lower and that of soft component to higher value.

**Table 2** Mechanical properties of ferrite grain in different crystallographic plane (in normal direction to the sample surface)

Steel	Mech. properties	(100)	(101)	(111)
XSG	H <sub>IT</sub> [MPa]	1670 ± 115	1784 ± 248	1761 ± 141
	E <sub>IT</sub> [GPa]	221 ± 28	230 ± 37	229 ± 16
HR 45	H <sub>IT</sub> [MPa]	1975 ± 183	2055 ± 162	2039 ± 182
	E <sub>IT</sub> [GPa]	245 ± 10	258 ± 4	256 ± 8

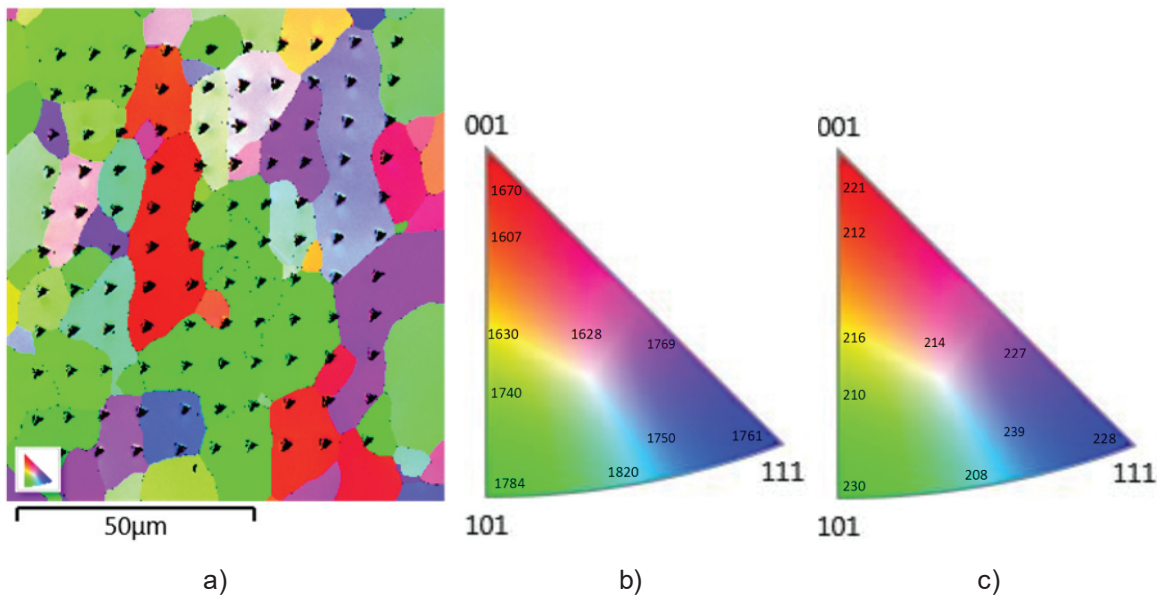


**Fig. 3** a) Indentation matrix in EBSD map of XSG steel, b) IPF of indentation hardness, c) IPF of Young's modulus (in direction normal to the sample surface)

**Fig. 4** shows effect of the rotation angle  $\varphi_2$  on hardness of ferrite grains. Detectable hardness anisotropy can be found as a function of rotation angle  $\varphi_2$ . The hardness increases with increasing rotation angle  $\varphi_2$ . Rotation angle  $\varphi_2$  has a similar effect on the hardness of ferrite grains in both XSG and HR 45 steel. XSG steel and HR 45 steel have the minimum hardness at rotation angle  $\varphi_2 = 10^\circ$ . Maximum hardness value of the ferrite grain in XSG steel is at rotation angle  $\varphi_2 = 42^\circ$  and in HR 45 steel it is at rotation angle  $\varphi_2 = 41^\circ$ .

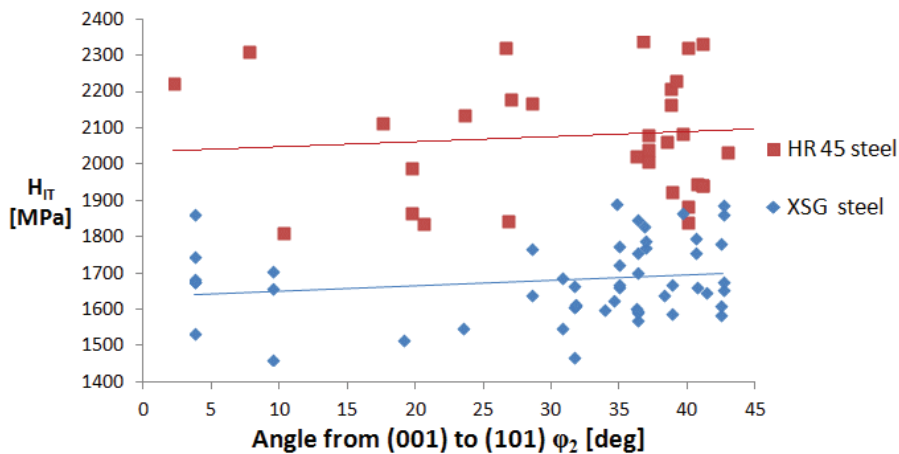


**Fig. 4** The hardness of ferrite grain as a function of grain orientation according to rotation angle  $\varphi_2$

#### 4. CONCLUSION

Mechanical properties of ferrite grains in the steel sheets are dependent on crystallographic orientation. Slip planes ((101), (111)) in body centred cubic grid have higher hardness and Young's modulus than plane (001). XSG steel and HR 45 steel have similar effect of crystallographic orientation on mechanical properties of ferrite grains. Mechanical properties of individual planes depend on grain size. The hardness increases with decreasing grain size.

#### ACKNOWLEDGEMENTS

*The paper was supported partly by the Project OP VaVpl Centre for Nanomaterials, Advanced Technologies and Innovation CZ.1.05/2.1.00/01.0005, partly by the Project Development of Research Teams of R&D Projects at the Technical University of Liberec CZ.1.07/2.3.00/30.0024 and partly by the VEGA project No. 1/0582/13 at the Technical University of Košice, Slovakia.*

#### REFERENCES

- [1] Information on: <http://hysitron.com/Portals/0/Updated%20Address/MET04AN%20r1.f.pdf>
- [2] HAUŠILD, P., MATERNA, A., NOHAVA J. Effect Crystallographic Orientation on Hardness and Indentation Modulus in Austenitic Stainless Steel. Key Engineering Materials, Vol. 586, 2014, pp. 31-34.
- [3] ZHOU X., JIANG Z., WANG H., YU R. Investigation on Methods for Dealing with Pile-Up Errors in Evaluating the Mechanical Properties of Thin Metal Films at Sub-micron Scale on Hard Substrates by Nanoindentation Technique. Materials Science and Engineering A, Vol. 488, 2008, pp. 318-332.
- [4] NOHAVA J., HAUŠILD P., RANDALL N.X. Grid Nanoindentation on Multiphase Materials for Mapping the Mechanical Properties of Complex Microstructures. IMEKO: TC3, TC5 and TC22 Conferences, Metrology in Modern Context, 2010, pp. 195-198.
- [5] RANDALL N.X., VANDAMME M., ULM F.J. Nanoindentation Analysis as a Two-Dimensional Tool for Mapping the Mechanical Properties of Complex Surfaces. Journal of Materials Research, Vol. 24, 2011, pp. 679-690.
- [6] ZOU J. Effects of Grain Size and Orientation on Mechanical Response of Lead Free Solders. 2013, Information on: [https://etd.auburn.edu/bitstream/handle/10415/3940/jingzou\\_thesis\\_r5.pdf?sequence=2](https://etd.auburn.edu/bitstream/handle/10415/3940/jingzou_thesis_r5.pdf?sequence=2)